V International Conference on Particle-based Methods – Fundamentals and Applications
PARTICLES 2017
P. Wriggers, M. Bischoff, E. Oñate, D.R.J. Owen, & T. Zohdi (Eds)

MODELLING OF THE DISPERSED PHASE MOTION IN FREE-SURFACE FLOWS WITH THE TWO-FLUID SMOOTHED PARTICLE HYDRODYNAMICS APPROACH

Michał Olejnik*, Kamil Szewc, Jacek Pozorski

Institute of Fluid Flow Machinery, Polish Academy of Sciences
Fiszera 14, 80-231 Gdańsk, Poland
*email: michal.olejnik@imp.gda.pl

Key words: Sedimentation, Free-surface Flow, Meshless Methods, Two-fluid Approach

Abstract. The sediment transport is an important problem in hydro-engineering. Accurate numerical modelling of this complex phenomenon remains a challenging task. In the present study we employ the Smoothed Particle Hydrodynamics (SPH) approach in the two-fluid formulation to compute the interactions between the carrier and dispersed phases. The main goal is to test this rather uncharted SPH variant for simple cases and to find problematic points that require further improvement. We present initial results of validation with experiment involving a vertical sheet of sand entering the water tank through free surface, as well as results from a simplified quasi-2D study of sedimentation.

1 INTRODUCTION

The phenomena involving interaction of the carrier fluid and dispersed phase are object of active research. In environmental sciences, transport of sediment (sand) in the coastal areas is a complex process of particular interest in hydro-engineering. Numerical predictions require advanced models able to handle physics of multiphase and free-surface flow. While some grid-based approaches to tackle this issue exist, they suffer from problems related to their Eulerian character. Lagrangian methods, such as Smoothed Particle Hydrodynamics (SPH), are surfacing as an interesting and promising alternative. Although initially the SPH method was developed for astrophysical computations, over the years it was successfully applied to a wide range of CFD problems, including both free-surface and multiphase flows [1, 2].

The present work is a part of ongoing development of entirely SPH-based solver capable of computing the free-surface flow, its interaction with deformable seabed [3], as well as transport of sand carried by water. In the following we focus on the last aspect. For this purpose we employ the so-called two-fluid SPH formulation, initially developed for calculations of dust motion within gaseous medium [4], recently adapted for sedimentation problems [5]. Basing on the results for the case of sand entering water through the free surface, as well as sedimentation problem, we outline main difficulties encountered.

2 GOVERNING EQUATIONS

2.1 Two-fluid model

The essence of the two-fluid modelling of multiphase flows is to treat the dispersed phase and the carrier fluid as two separate continuous phases, interpenetrating and interacting with each other. As a consequence the conservation equations for both phases, including interaction terms between them, are solved. The idea of this approach can be found in [6]. In this work we consider liquid L and dispersed phase (dust) D. Their volume densities are defined as

$$\hat{\varrho}_L = \theta_L \varrho_L, \tag{1}$$

$$\hat{\varrho}_D = \theta_D \varrho_D, \tag{2}$$

where θ and ϱ denote the volume fraction and material density, respectively. The volume fractions need to satisfy the condition

$$\theta_L + \theta_D = 1. \tag{3}$$

The mass conservation equation for each phase is given as

$$\frac{d\hat{\varrho}_L}{dt} = -\hat{\varrho}_L \nabla \cdot \mathbf{u}_L, \tag{4}$$

$$\frac{d\hat{\varrho}_D}{dt} = -\hat{\varrho}_D \nabla \cdot \mathbf{u}_D, \tag{5}$$

and the momentum conservation equations are

$$\frac{d\mathbf{u}_L}{dt} = -\frac{\nabla p}{\varrho_L} - \frac{K}{\hat{\varrho}_L}(\mathbf{u}_L - \mathbf{u}_D) + \frac{1}{\varrho_L}(\nabla\mu \cdot \nabla)\mathbf{u}_L + \mathbf{f}, \tag{6}$$

$$\frac{d\mathbf{u}_D}{dt} = -\frac{\nabla p}{\varrho_D} - \frac{K}{\hat{\varrho}_D}(\mathbf{u}_D - \mathbf{u}_L) + \mathbf{f}, \tag{7}$$

where $\mathbf{f}$ and K denote the mass force and the drag factor, respectively; μ is the dynamic viscosity. An example of the two-fluid approach calculations within Eulerian-Eulerian framework for problem of a dust sedimentation can be found in [7]. Since our long-term aim is to include the effect of surface waves on the dispersed phase, as well as the specific model of the bottom layer [3], we decided to apply the Lagrangian-Lagrangian two-fluid model, based on a particle method, namely SPH.

2.2 SPH formulation

The general idea behind SPH lies in interpolation theory. Let us consider any scalar (for simplicity) field A. The integral formula

$$A(\mathbf{r}) = \int_\Omega A(\mathbf{r}')\delta(\mathbf{r} - \mathbf{r}')\mathbf{d}\mathbf{r}', \tag{8}$$

where $\delta(\mathbf{r})$ is the Dirac delta function, can be used to express the field value at the point $\mathbf{r}$ in space Ω. To obtain SPH approximation, first we replace $\delta(\mathbf{r})$ with the weighting kernel function $W(\mathbf{r}, h)$ which should be normalised, symmetrical and converge to $\delta(\mathbf{r})$ with $h \to 0$ [1]. Argument h is the so-called smoothing length and it determines the interpolation range. In our work we use the Wendland kernel [8], as the one guaranteeing good stability of computations [9].

The second step consists in discretisation of space into a set of particles of volume $\Omega_b = m_b/\varrho_b$, where m_b is the mass and ϱ_b is the density of particle b. As a result the integral from Eq. (8) is approximated by a sum, i.e.

$$A(\mathbf{r}) \simeq \sum_b A(\mathbf{r}_b)W(\mathbf{r} - \mathbf{r}_b, h)\Omega_b. \tag{9}$$

In the shorthand notation, the SPH approximation $\langle A\rangle_a$ of field A at any point a is defined as

$$\langle A\rangle_a = \sum_b A_b W_{ab}(h)\Omega_b, \tag{10}$$

where $A_b = A(\mathbf{r}_b)$ and $W_{ab}(h) = W(\mathbf{r}_a - \mathbf{r}_b, h)$. Thanks to the properties of $W(\mathbf{r}, h)$ differentiation can be shifted from the field to the kernel function yielding

$$\langle \nabla A\rangle_a = \sum_b A_b \nabla W_{ab}(h)\Omega_b. \tag{11}$$

Further derivatives can be obtained in a similar way. Using Eqs. (10) and (11) differential equations can be rewritten in SPH formalism and solved by calculating interaction between particles. The detailed derivation of the SPH method for fluid-flow problems can be found in [2].

Now, we will briefly recall the two-fluid SPH formulation used in the present study. In this approach both phases are described by separate sets of SPH particles. Following the original work by Monaghan and Kocharyan [4] we denote liquid particles with indices a and b, while i and j are used for the dust particles. We recall that the "dust particles" are understood here as parts of the continuum, and not the real physical particles. Since cases considered in this research involve free-surface flows, we decided to use SPH formalism proposed by Colagrossi and Landrini [10], well suited for the task [11]. In this formulation Eqs. (4) and (5) will become

$$\frac{d\hat{\varrho}_a}{dt} = -\hat{\varrho}_a \sum_b \frac{m_b}{\hat{\varrho}_b}\mathbf{u}_{ab} \cdot \nabla_a W_{ab}, \tag{12}$$

$$\frac{d\hat{\varrho}_i}{dt} = -\hat{\varrho}_i \sum_j \frac{m_j}{\hat{\varrho}_j} \mathbf{u}_{ij} \cdot \nabla_i W_{ij}, \tag{13}$$

where $\mathbf{u}_{ab} = \mathbf{u}_a - \mathbf{u}_b$. Equations (6) and (7) are taken as

$$\begin{aligned} \frac{d\mathbf{u}_a}{dt} = \sum_b m_b \left(\frac{\theta_a p_a + \theta_b p_b}{\hat{\varrho}_a \hat{\varrho}_b} + \Pi_{ab} \right) \nabla_a W_{ab} - \sum_j m_j \frac{\theta_j p_a}{\hat{\varrho}_a \hat{\varrho}_j} \nabla_a W_{aj} + \\ -\sigma \sum_j m_j \frac{K_{aj}}{\hat{\varrho}_a \hat{\varrho}_j} (\mathbf{u}_{aj} \cdot \hat{\mathbf{r}}_{aj}) \hat{\mathbf{r}}_{aj} W_{aj} + \mathbf{f}, \end{aligned} \tag{14}$$

$$\begin{aligned} \frac{d\mathbf{u}_i}{dt} = \sum_j m_j \left(\frac{\theta_i p_i + \theta_j p_j}{\hat{\varrho}_a \hat{\varrho}_b} \right) \nabla_i W_{ij} - \sum_b m_b \frac{\theta_i p_b}{\hat{\varrho}_i \hat{\varrho}_b} \nabla_i W_{ib} + \\ -\sigma \sum_b m_b \frac{K_{ib}}{\hat{\varrho}_i \hat{\varrho}_b} (\mathbf{u}_{ib} \cdot \hat{\mathbf{r}}_{ib}) \hat{\mathbf{r}}_{ib} W_{ib} + \mathbf{f}, \end{aligned} \tag{15}$$

where σ (2 or 3) is the dimensionality of the problem. The first two r.h.s. terms in the above equations are the pressure terms, with Π being the viscous stress tensor for liquid phase. The third term is the drag term. To calculate the drag coefficient, Gidaspow's drag model [12] is used in which

$$K = \begin{cases} 150 \frac{\theta_D^2}{\theta_L^2} \frac{\mu}{d^2} + 1.75 \frac{\theta_D}{\theta_L} \frac{\varrho_L}{\varrho_D} |\mathbf{u}_{LD}| & \text{when} \quad \theta_L < 0.8 \\ \frac{3 \varrho_L \theta_L \theta_D C_D}{4d} |\mathbf{u}_{LD}| \theta_L^{-2.65} & \text{when} \quad \theta_L \geq 0.8 \end{cases}. \tag{16}$$

where d is the diameter of solid particle and C_D is drag coefficient taken as [13]

$$C_D = \frac{24}{Re_p} \left(1 + \frac{3}{16} Re_p \right)^{0.5}, \tag{17}$$

and $Re_p = d|\mathbf{u}_{LD}|/\nu$. The slip velocity $\mathbf{u}_{LD}$ is defined as $\mathbf{u}_{LD} = \mathbf{u}_L - \mathbf{u}_D$. The liquid-dust interactions used in the evaluation of drag term are calculated using a double-hump-shaped kernel

$$W(q) = \frac{63}{320\pi} q^2 (1 + 2q)(2 - q)^4, \tag{18}$$

where $q = |\mathbf{r}|/h$, $q \leq 2$. The liquid volume fraction is calculated from

$$\frac{d\theta_a}{dt} = -\frac{1}{\varrho_D} \sum_j m_j \mathbf{u}_{aj} \cdot \nabla_a W_{aj}, \tag{19}$$

and Eq. (2) for the dispersed phase [5]. The set of governing equations for fluid flow is closed with the state equation in the form

$$p_a = \frac{s^2 \varrho_0}{\gamma} \left[\left(\frac{\varrho_a}{\varrho_0} \right)^{\gamma} - 1 \right], \tag{20}$$

Figure 1: Left picture: test of the sand dispenser (the mass flux measurement in "dry" conditions). Right picture: the laser-lit sand sheet falling in the water tank; the upper edge marks the free surface and the white dashed line indicates the border of the sand-laden area; the sand bottom visible as lighter-gray region. Experimental data, courtesy of B. Stachurska (IBW PAN).

where s is a numerical speed of sound, γ is a constant and ϱ_0 is a reference density. In the present work, we deal with small volume fractions of dispersed phase, i.e. $\theta_D \leq 0.2$, hence we assumed $p_i = 0$ for all dust particles.

Note that, contrary to the original works where this model was developed [5, 14], all interactions are calculated using constant smoothing length. Additionally we use equation for mass evolution

$$\frac{dm_a}{dt} = m_a \sum_b \frac{m_b}{\hat{\varrho}_b} \mathbf{u}_{ab} \cdot \nabla_a W_{ab}, \tag{21}$$

to correct possible issues generated by changing volume densities, for details see [11].

3 RESULTS

3.1 Validation with the experiment

Since the model was tested for the cases of sedimentation in static and stirred tank [5, 14], we decided to proceed with validation with experiment designed and conducted specially for this task. The main goal was to deliver results that could serve as reference data for 2D numerical simulation. For that purpose, a simple wooden box with a thin outlet slit was constructed to form the curtain of sand with the width of 400 mm and the nominally constant thickness, in practice varying from 3 to 5 mm, see left panel of Fig. 1. The sand used had density of 2650 kg/m^3 and the mean grain diameter of 0.26 mm, and the measured mass flux was 148 ± 7 g/s. In the experiment, the sand sheet was vertically poured into the water tank, large enough to neglect the influence of vertical walls. Particle image velocimetry (PIV) measurements of the velocity field were performed with sand grains as tracers. A single experimental run lasted 10 seconds, measured from

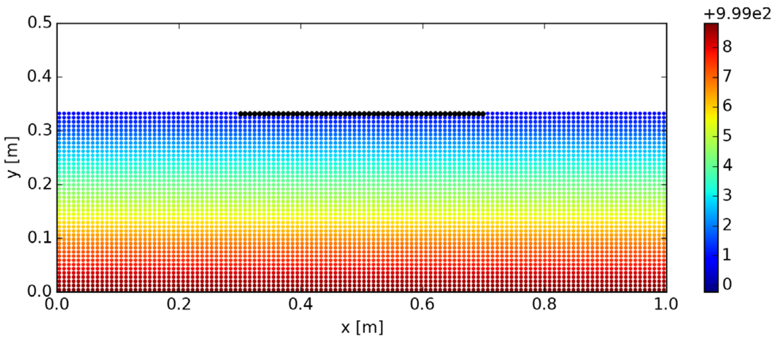

Figure 2: Computational domain at $t = 0\,\mathrm{s}$. Fluid particles are coloured with their densities set to match the hydrostatic pressure; black particles represent the sand.

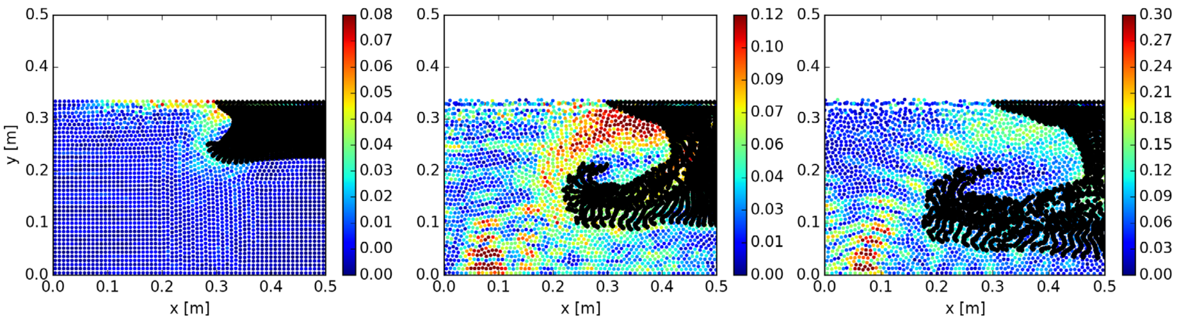

Figure 3: The SPH computation at $t = 2.5\,\mathrm{s}$ (left), $t = 5\,\mathrm{s}$ (middle) and $t = 6\,\mathrm{s}$ (right). Fluid particles are coloured with their velocities, black particles represent the sand; only the left half of domain is shown since the flow case was symmetric in practice, see Fig. 4.

the opening of the sand source to its closure. While the whole setup was designed to be treated as 2D case, dispersion of sand in direction perpendicular to the curtain's width was inevitable, making it in fact a 3D problem.

To reconstruct the experimental setup within the numerical simulation we used a square computational domain with periodic boundary conditions in the horizontal direction and no-slip boundary modelled with ghost particles at the bottom for the liquid phase. In the case considered, the initial water level was set to 33 cm, with one row of the dust particles at the free-surface, see Fig. 2. Initial velocity of dust was set to $u_0 = 25\,\mathrm{cm/s}$ as in the experiment. The new row of particles was added at the same place every 0.1 s with their velocities set to u_0. Due to the lack of proper boundary conditions at the bottom for dispersed phase, the dust particles were made to stop after reaching it.

The main problem in reconstructing the experimental conditions lies in setting θ_D, so that its value and the mass flux of sand are the same as in experiment. As a temporary remedy we tried to set θ_D, so that the mass flux is match, i.e. after 1 s mass of sand in the domain is equal to 148 g, which corresponds to $\theta_D = 0.00176$ at the resolution of

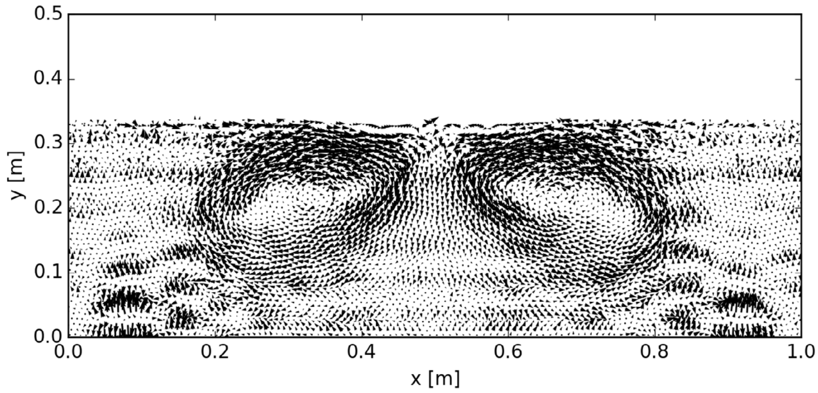

Figure 4: Velocity field of the liquid phase at $t = 5\,\mathrm{s}$ (see Fig. 3).

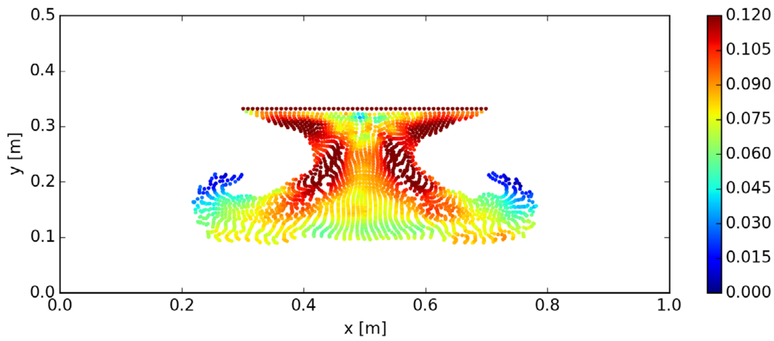

Figure 5: Velocity magnitude of dust particles at $t = 5\,\mathrm{s}$ (see Fig. 3).

$L/h = 64$ and $h/\Delta r = 2$. This turned out to be not the best solution, since such a low volume fraction of the dispersed phase had barely any effect on the liquid and general outcome was much different from the experimental one.

Setting θ_D to 0.0176 yielded more interesting results. Obviously, the mass flux was too high (1.48 kg/s), but this volume fraction was enough to stir the fluid, see Fig. 3. This resulted in two vortices appearing at the edges of sedimenting sand curtain, see Fig. 4. Note, that the velocity field within the liquid was rather noisy, especially in later stages of simulation.

It is hard to compare these results with the reference data, since the initial conditions were not reproduced perfectly. For the case of higher θ_D the behaviour of sand, i.e. bending of sand sheet near the free surface into a triangular shape and later expansion, was similar to the observations made in experiment, see right panel of Fig. 1. Furthermore, PIV measurements showed that sedimentation velocity was higher in the outer parts of sand curtain. This effect was also reproduced in SPH simulation, as shown in Fig. 5. It is important to note that rough estimations of θ_D in the experiment point towards

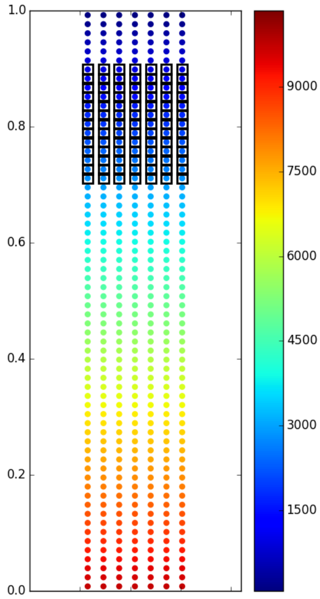

Figure 6: Computational domain at $t = 0$ s for quasi-2D simulation. Liquid particles are coloured with the hydrostatic pressure, dust particles are marked with black squares.

values around 0.1; however, reproducing this in calculations would require much higher resolution to reproduce mass flux correctly.

3.2 Quasi-2D study of sedimentation

Not satisfied with noisy velocity field within the liquid phase, see Fig. 3, we decided to investigate the model in more detail. For that purpose we used the validation case described by Kwon and Monaghan, 2015 [5], i.e. the infinitely long layer of sediment of thickness $0.2H$ falling due to the gravity within a hydrostatic tank of height H. Usually, periodic boundary conditions would be used, but since there is no motion in the x direction, governing equations can be solved with only y component. To avoid deriving the 1D SPH formulation, we considered 7 columns of particles, and solved governing equations for the middle one; for the initial setup see Fig. 6. Thanks to the compact support of the weighting kernels used, interactions with particles further away would return zero values. After the advection step, the fields' values and particle positions are rewritten row by row with those from the 4th column, hence quasi-2D. The sediment is placed between $0.7H$ and $0.9H$. Due to the gravity it should start falling and after short time reach constant settling velocity v_{ref}, known from the analytical solution of the problem. The results reported in this paper were obtained for $\theta_D = 0.02$ in the area occupied initially by dust; similar outcomes and conclusions were obtained for higher values of this parameter, however, we omitted them in the following for clarity.

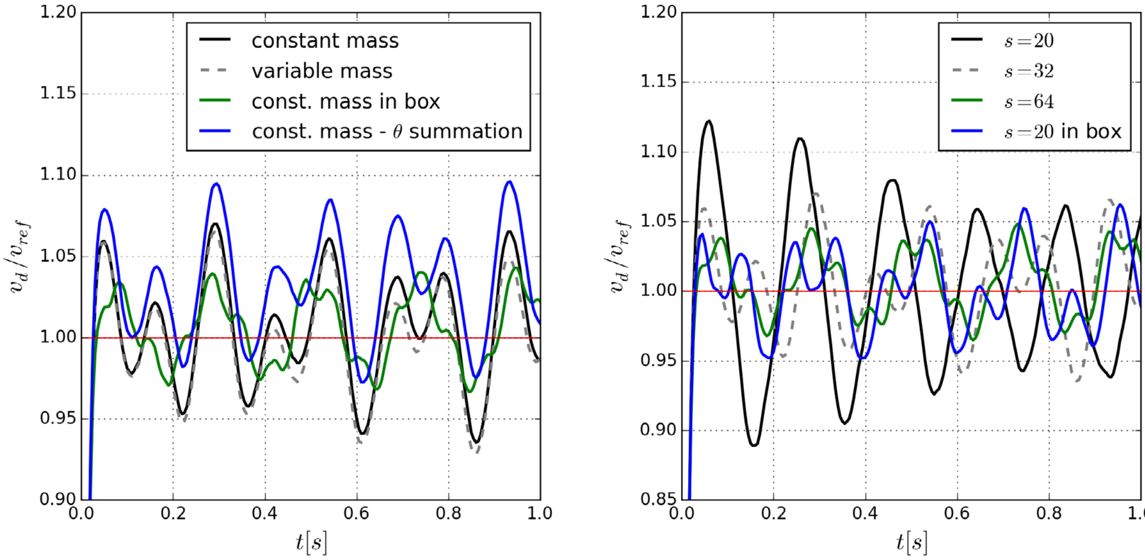

Figure 7: Evolution of the mean settling velocity for different variants of the model with $s = 32$ m/s (left) and influence of this parameter for the constant mass one (right).

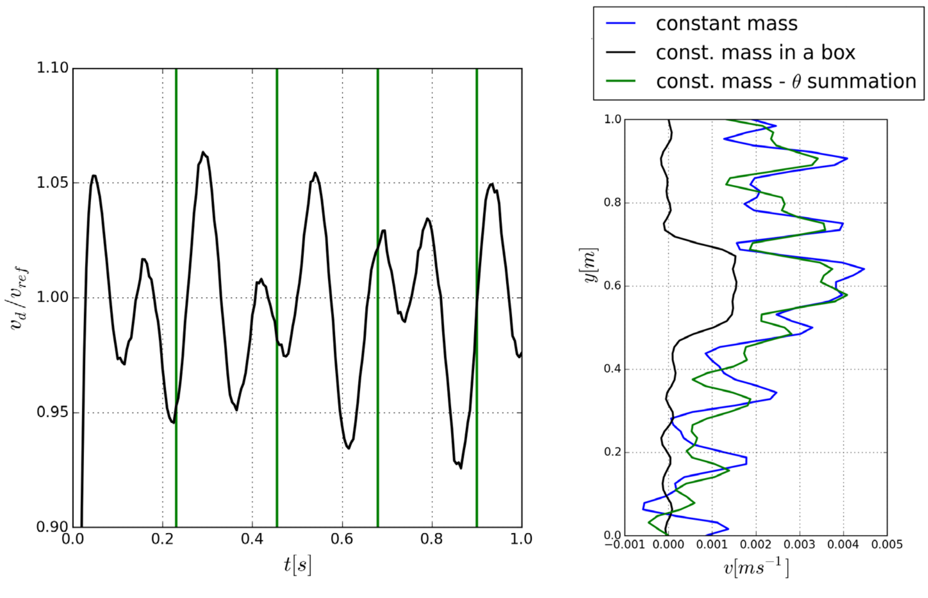

Figure 8: Evolution of the mean settling velocity for the middle row of dust particles with horizontal lines marking timesteps at which they are passing right through liquid particles (left) and comparison of the liquid phase velocity profiles (right).

For the sake of comparison we tested different variants of the model, namely:

1) "constant mass" - model presented in Section 2.2 without Eq. (21),

2) "variable mass" - model presented in Section 2.2 with Eq. (21),

3) "constant mass in box" - the same as the 1st one but with domain closed with wall instead of free surface,

4) "constant mass - θ summation" - the same as the 1st one but with summation formula for θ_L

$$\theta_a = 1 - \frac{1}{\varrho_D} \sum_j m_j W_{aj}, \tag{22}$$

instead of Eq. (19).

The result for the evolution of settling velocity v_d averaged over all dust particles is shown in Fig. 7. The velocity, instead of reaching a constant value, oscillates around the analytical prediction. Using Eq. (21) does not improve the results significantly, while the variant with evolution equation for θ_L gives slightly more accurate result. The magnitude of oscillations is lowered by increasing the speed of sound in Eq. (20), but without affecting their frequency. Closing the domain with the upper wall, however, improves outcomes in most visible way. It reduces the magnitude of oscillations, even for the lowest value of s tested. One of the possible reasons for this oscillations could be interaction of two sets of particles passing through each other, however, as presented on the left plot of Fig. 8, there is now correlation between extrema of the value of v_d and moments when dust particles are positioned exactly at spots occupied by the liquid particles. Furthermore, comparison of velocity profiles of water, see right plot of Fig. 8, shows that closing domain with the lid significantly reduces noise. This solution, while simple, is not very practical since it restricts simulations only to internal flows. The reason for oscillations in sedimentation velocity is hard to be pin-pointed, however, the fact that closed domain improves the results implies that the "liquid" part of the two-fluid SPH formulation requires some improvement for the free-surface flows.

4 CONCLUSIONS

In the paper the performance the two-fluid SPH model was assessed. The comparison with experiment was not complete due to difficulties in exact reproduction of the initial conditions within numerical simulation. The qualitative results, however, showed that the motion of the sand within a water computed with SPH was very similar to that observed in experiment. The analysis of the results for sedimentation in the quasi-2D setup showed that, apart from hard to explain oscillations in dust settling velocity, the formulation used for calculations requires a further extension of the model to treat free-surface flows. Using some variation of the δ-SPH scheme [15] might be one of the possible solutions.

Nevertheless, the perspective is promising, especially considering recent advancements in SPH for granular flows [3] and possible coupling of different SPH formalisms for hydro-engineering calculations.

Acknowledgements

This research was supported by the National Science Centre, project No. 2013/11/B/ST8/03818. We would like to thank Barbara Stachurska and Professor Ryszard Staroszczyk from Institute of Hydroengineering, Polish Academy of Sciences (IBW PAN) for providing the experimental data.

REFERENCES

[1] Monaghan, J.J., Smoothed Particle Hydrodynamics, *Annu. Rev. Astron. Astrophys.*, 30, pp. 543-574, 1992.

[2] Violeau, D. *Fluid Mechanics and the SPH Method: Theory and Applications*. Oxford University Press (2012).

[3] Szewc, K. Smoothed particle hydrodynamics modelling of granular column collapse. *Granul. Matter* (2017) **19:3**:1-13.

[4] Monaghan, J.J. and Kocharyan, A. SPH simulation of multi-phase flow. *Comp. Phys. Comm.* (1995) **87**:225-235.

[5] Kwon, J. and Monaghan, J.J. Sedimentation in homogeneous and inhomogeneous fluids using SPH. *Int. J. Multiphase Flow* (2015) **72**:155-164.

[6] Brennen, C.E. *Fundamentals of Multiphase Flows*. Cambridge University Press (2005).

[7] Bergantz, G.W. and Ni, J. A numerical study of sedimentation by dripping instabilities in viscous fluids. *Int. J. Multiphase Flow* (1999) **25**:307-320.

[8] Wendland, H. Piecewise polynomial, positive definite and compactly supported radial functions of minimal degree. *Adv. Comput. Math.* (1995) **4**:389-396.

[9] Szewc, K., Pozorski, J., and Minier, J.-P., Analysis of the incompressibility constraint in the SPH method, *Int. J. Numer. Meth. Eng.*, (2012) **92**:343-369.

[10] Colagrossi, A. and Landrini, M. Numerical simulation of interfacial flows by smoothed particle hydrodynamics. *J. Comput. Phys.* (2003) **191**:227-264.

[11] Szewc, K. Fluid-granular media multiphase modelling using the Smoothed Particle Hydrodynamics method. *9th International Conference on Multiphase Flow*, Florence, Italy, May 22-27, 2016, paper no. **1098**, Proceedings on a USB.

[12] Gidaspow, D. *Multiphase Flow and Fluidization: Continuum and Kinetic Theory Description*. Academic Press, San Diego (1994).

[13] Olson, R.M. *Essentials of Engineering Fluid Mechanics*. International Textbook Company, Scranton, Pennsylvania (1960).

[14] Kwon, J. and Monaghan, J.J. A novel SPH method for sedimentation in a turbulent fluid. *J. Comp. Phys.* (2015) **300**:520-532.

[15] Molteni, D. and Colagrossi, A. A simple procedure to improve the pressure evaluation in hydrodynamic context using the SPH. *Comp. Phys. Comm.* (2009) **180**:861-872.